Construction of a minicellulosome-producing consolidated bioprocessing reaction system for simultaneous saccharification and co-fermentation from Pennisetum purpereum

Han Liu
Jiliang Du
Xuxin Wang
Zhuoran Kang
Chenglin Hou
Xiushan Yang
Shen Tian (cnu_tianshen@sina.com)

Research Article

Keywords: Hemicellulosome, Simultaneous saccharification and co-fermentation, Cellulosic ethanol, Consolidated bioprocessing, Saccharomyces cerevisiae

Posted Date: May 11th, 2022

DOI: https://doi.org/10.21203/rs.3.rs-1613391/v1

Abstract

The enhanced hydrolysis of xylan-type hemicellulose is important to maximize ethanol production yield and substrate utilization rate in lignocellulose-based simultaneous saccharification and co-fermentation system. In this study, we conduct d-integration CRISPR Cas9 to achieve multicopy chromosomal integration with high efficiency of reductase-xylitol dehydrogenase pathway in *Saccharomyces cerevisiae*. Subsequently, a mincellulosome attaching with hemicellulose-degrading enzymes on this xylose-utilizing recombinant yeast strain is developed for synergistic catalysis and co-fermentation from steam-exploded *Pennisetum purpereum*. Despite the accumulation of xylitol, the maximum ethanol titer of genetic engineered yeast strain reached 4.77 g/l with the cellulose conversion of 97.02% and hemicelluose conversion of 67.45% under 30 ºC after 96 h with the addition of commercial cellulase. The elaborated cellulosomal organization toward genetic engineering of an industrially important microorganism presents a designed approach for advanced lignocellulolytic potential and improved capability of biofuel processing.

1. Background

Second generation bioethanol, produced by available sugars present in renewable lignocellulosic feedstock is a promising alternative biofuel due to the diverse and abundance of resources available. It is well known that the perennial C4 grass is sustainable feedstock for biofuel production, since it can avoid the competition with food crops because of its high photosynthesis ability and extensive environmental adaptability [1]. However, one of the main bottlenecks in achieving a competitive and economically feasible lignocellulose-based bio-refinery with broadened productive character is the current technological impediments to improve production yield and bioconversion efficiency.

Co-fermentation of pentose and hexose through the simultaneous saccharification and microbial metabolism process of biomass is realized to be a significantly important strategy for a competitive lignocellulosic biorefinery and economically feasible. *Saccharomyces cerevisiae* is the classic industrial microorganism with native capacity to produce ethanol, thus it is generally utilized as the ideal host cell for engineering genetic strain to perform the simultaneous assimilation of glucose and xylose [2]. Till so far, efficient biofuel conversion for meeting the needs of industrial application from lignocellulosic materials remains challenges despite a lot of efforts have been made for process optimization and integration in biomass-refinery. Few reports have demonstrated an ideal bioconversion rate based on holocellulose (cellulose + hemicellulose).

The efficient hydrolysis of xylan-type hemicellulose, consequently, has been a major focus in in *S. cerevisiae* strain-engineering of simultaneous saccharification and co-fermentation (SSCF) for maximizing both utilization rate and production yield [3]. Xylan representing the main hemicellulose component of biomass is a polysaccharide formed by units of xylose as the backbone with β-1,4 linkages, partially substituted with arabinose, uronic acids and acetyl groups, which can be hydrolysed into xylooligosaccharides and xylose by xylanases and xylosidases [4, 5]. These hydrolytic products, however, cannot be metabolized by the wildtype *S. cerevisiae*. Therefore, a promising recognition of consolidated bioprocessing (CBP) for whole-cell catalysis, which combines different functional enzymes of xylan-degrading and xylose-assimilating in one yeast strain, emerges as a novel configuration to SSCF process for direct cellulosic ethanol bioconversion [6, 7]. CBP-microorganism could be described as a sustainable biocatalyst that presents higher catalytic efficiency and better substrate selectivity due to its utility in cofactor regeneration, and multistep reactions can be carried out in single strain under milder operational conditions. As one of the most robust and intricate molecular nanomachine, cellulosome serves to facilitate synergistic activity and enhanced close proximity among different enzymatic systems, which conduct enhancing hydrolysis of lignocellulose [8]. Hence, utilizing cellulosome as a functional resource for construction of CBP-enabling microbial strain is required. Several developments of engineered cellulolytic complex attaching with cellulosomal enzymes have been reported in the past [9, 10, 11]. However, “chimeric hemicellulases and mini-hemicellulosome” have few been employed in “arming yeast” strategy for simultaneous hydrolysis and co-fermentation of pentose and hexose.

In this work, to construct the engineered *S. cerevisiae* with enhanced xylose catabolism by introducing xylose reductase (XR)-xylitol dehydrogenase (XDH) pathway, we harnessed Di-CRISPR (Delta-integration CRISPR-Cas9) to specifically generate double strand breaks at the δ-sites in yeast genome to increase the recombination efficiency of *XYL1* and *XYL2*, encoding for xylose reductase and xylitol dehydrogenase, respectively. On the basis of the construction of xylose-utilizing *S. cerevisiae* strain, the aim of the present study was: (1) demonstrate the potential of xylose-fermenting *S. cerevisiae* as the host for engineering of synthetic minicellulosome attaching with xylan-hydrolysing enzymes together with the heterologous expression of XR and XDH; (2) evaluate the efficiency of this lignocellulose-based CBP system of simultaneous saccharification and co-fermentation in terms of holocellulose bioconversion from pretreated *Pennisetum purpereum*, a perennial C4 grass.

2. Materials And Methods

2.1 Raw materials

The *Pennisetum purpereum* was obtained from Guangzhou Institute of Energy Conversion, CAS. The materials were pretreated by steam explosion at 1.6Mpa and 195℃ for 5 minutes (Institute of Process Engineering, CAS). The pretreatment material was used as SSCF substrate without detoxification. The major chemical composition including lignin and structural carbohydrates of treated and untreated grass was summarized (table 1) and analyzed following NREL standard analytical procedure (TP-510-42,618).

Table 1

Main chemical compositions of untreated and treated *Pennisetum purpereum* (% of DM).

Materials	Cellulose (glucan)	Hemicellulose (xylan and arabinan)	Lignin[b]	Ash	Extractives + Others[c]
Unpretreated[a]	35.2 ± 0.38	25.0 ± 3.74	20.1 ± 1.33	7.5 ± 0.20	12.2 ± 0.21
Pretreated[a]	48.7 ± 0.41	8.3 ± 0.19	29.4 ± 0.38	8.2 ± 0.01	5.4 ± 0.30
All values are averages ± standard deviation of three independent experiments.					
[a] Data shown as percentage of dry matter (DM)					
[b] Acid-soluble lignin included					
[c] Non-structural material and other compounds from biomass					

2.2 Strains and media

Saccharomyces cerevisiae haploid strain Y6 (*MATa ade2-1 can1-100 his3-11,15 leu2-3,112 trp1-1 ura3-1*) was used as the host for xylose metabolic pathway engineering by introducing *XYL1*, *XYL2* genes of *Pichia stipitis*, thus generating a xylose-utilizing strain that was then utilized to display adaptor scaffoldin and assemble minicellulosome architecture. Strains and plasmids used in this study are listed in Table 2. Yeasts were routinely maintained in yeast extract peptone dextrose (YPD) medium containing 2% glucose. All yeast transformants were selected and maintained on synthetic dropout nutrient medium (SD-Ura/-Trp). *Aspergillus oryzae* 2120 and *Trichoderma reesei* 40358 were purchased from Industrial Culture Collection Center of China. *Clostridium thermocellum* ATCC 27405 was purchased from DSMZ (Germany). All DNA manipulations were performed in *Escherichia coli* DH5α, which grown in Luria Bertani (LB) broth with 10 mg/L ampicillin.

2.3 DNA manipulation and plasmid construction

The recombination plasmid pDi-CRISPR for δ-integration CRISPR-Cas9 was designed and modified from the pCRCT plasmid (Beijing Zoman Biotechnology Co., Ltd) with specific delta Cas9-gRNA, which mediates Cas9 protein targeting the delta sequence to generate specific double stranded breaks (DSBs). The gRNA1-F/gRNA1-R was incubated to form duplex DNA encoding the specific delta Cas9-gRNA. The gRNA sequence was inserted into the *Bsa*I site of pCRCT to generate pDi-CRISPR, and it was then verified by sequencing.

The *XYL1* (GI: X59465) and *XYL2* (GI: XM_001386945) encoding for xylose reductase and xylitol dehydrogenase were obtained from the genomic DNA of *Pichia stipitis*. 5′δ and 3′δ, each containing flanking δ-sequence segments were obtained from *S. cerevisiae* Y6 genomic DNA. Two DNA expression cassettes: 5′δ-PGK-XR-Matt-3′δ and 5′δ-PGK-XDH-Matt-3′δ were both individually over-lap PCR amplified with homologous arms and purified (Universal DNA pure Kit, BGI, China).

For δ-integration CRISPR-Cas9, 300 ng each of DNA cassettes was mixed with 1 μg pDi-CRISPR and transformed into *S. cerevisiae* strain Y6 to generate $Y6^{g}$/XR-XDH strain. In the control group, the same operation was carried out for conventional δ-integrated assembly via donor DNA fragments without CRISPR Cas9 mediation to generating a control strain $Y6^{\delta}$/XR-XDH. More detailed information about plasmid construction was summarized in the supplementary information.

The genes encoding two specific cohesin domains, *SdbA* (GI: AAB07763.1) and *OlpA* (GI: Q06848.1), were from *Clostridium thermocellum* ATCC 27405. The two genes were spliced into a fusion gene fragment *ScafI* by over-lap PCR. *SacfI* was digested and cloned into 3′-terminal of AGA2 gene in plasmid pYD1-PGK-AGA2 to generate the cell-surface displaying plasmid of anchoring scaffoldin. The anchoring scaffoldin ScafI was labeled with C-terminal Xpress tag. The DNA sequence of secretion signal α-factor was cloned from plasmid pPIC9K to construct enzyme secretion plasmid pYD1-PGK-αMF. The genes of the xylosidase (*XylA*, GI: AB013851.1) of *A. oryzae* and the endoxylanase (*XynII*, GI: U24191.1) of *Trichoderma reesei* were 3′-terminal fused with the dockerin sequence OlpA and SdbA, respectively. Then they were digested and cloned into pYD1-PGK-αMF for constructing xylanases secretion-expressed plasmids pYD1-XylA-OlpA and pYD1-XynII-SdbA. Both DNA fragments of XynII-SdbA and XylA-OlpA were designed to contain a C-terminal 6×His tag for western-blot assay.

The plasmids of pYD1-ScafI, pYD1-XylA-OlpA and pYD1-XynII-SdbA were co-transformed into strain $Y6^{g}$/XR-XDH to obtain recombination strain $Y6^{g}$/ScafI-XylA-XynII. The yeast transformations were performed using the standard lithium acetate procedure. All recombinant yeast strains used in this study are summarized in Table 2.

Table 2
Summary of the recombinant *S. cerevisiae* strains used in this study.

Plasmid/Strain	Genotype/Property	Resource
Saccharomyces cerevisiae		
Y6	MATa{leu2-3,112 trp1-1 can1-100 ura3-1 ade2-1 his3-11,15}	Tian, 2019
$Y6^{\delta}$/XR-XDH	{5'δ-PGK-XR-MATT-3'δ; 5'δ-PGK-XDH-MATT-3'δ}, based on traditional delta integration	This work
$Y6^{g}$/XR-XDH	{5'δ-PGK-XR-MATT-3'δ; 5'δ-PGK-XDH-MATT-3'δ}, based on delta integration enhanced by CRISPR	This work
$Y6^{g}$/ScafI	Surface displaying the achoring scaffoldin ScafI on the cell of $Y6^{g}$/XR-XDH	This work
$Y6^{g}$/XylA	Expression of catalytical module XylA containg dockerin OlpA by $Y6^{g}$/XR-XDH	This work
$Y6^{g}$/XynII	Expression of catalytical module XynII containg dockerin SdbA by $Y6^{g}$/XR-XDH	This work
$Y6^{g}$/ScafI-XylA-XynII	Surface displaying the hemicellulosomal complex attaching with dockerin-containing XylA and XynII on the cell of $Y6^{g}$/XR-XDH	This work
Plasmids		
pYD1	Ori, GAL1, Aga2, Amp, Trp3	Commercial
pYD1-PGK-αMF	Ori, PGK, αMF, Amp, Trp3	Tian, 2019
pCRCT	Ura3, encoding iCas9, tracrRNA and crRNAs	Commercial
pDi-CRISPR	Ura3, encoding iCas9, gRNA targeting δ sequence from pCRCT	This work
pYD1-ScafI	pYD1, PGK-Aga2-ScafI-MATT, Amp, Trp3	This work
pYD1-XylA-OlpA	pYD1, PGK-αMF-XylA-OlpA-MATT, Amp, Trp3	This work
pYD1-XynII-SdbA	pYD1, PGK-αMF-XynII-SdbA-MATT, Amp, Trp3	This work

2.4 Copy number determination of XR-XDH pathway

The integrated gene copy numbers of recombinant strains were determined by real-time quantitative PCR (RT-qPCR) using the yeast genomic DNA. The *XYL1*, *XYL2* of site-specific integration and *S. cerevisiae ALG9* gene were chosen as the target gene and reference gene, respectively. The plasmid containing reference gene or target gene was used to generate the standard curves. The relative copy numbers of the target genes were determined by comparing them with the reference gene [12]. Real-time qPCR reactions were performed using *PerfectStart*® Green qPCR SuperMix (TransGen Biotech, China) on a BioRad CFX96 Touch real time PCR system.

2.5 Enzyme assay

The hemicellulases-producing yeasts were grown in YPD medium at 30 °C for 48 h before centrifuging the cultures at 4000 rpm for 5 min at 4°C. Endoxylanase activity was determined by dinitrosalicylic acid (DNS) method [13]. Add the supernatant into the reaction mixture containing 50 mM Tris-HCl buffer (pH 5.5) and 0.5% specified substrate at 45°C for 20 min, then add DNS and boil for 10 min. The concentration of xylose was measured by detecting absorbance value of enzyme reaction mixture at 540nm. The amount of enzyme required to produce 1 mg xylose per hour under the above conditions is defined as enzyme-activity unit. Xylosidase activity was measured in 50 mM sodium citrate buffer (pH 5.0) with 5 mM 4-nitrophenyl β-D-xylopyranoside (*p*NPX) as substrate for 10 min at 30°C. One unit of enzyme activity is defined as 1 μM liberated sugar from substrate per minute by measuring at $OD_{405\,nm}$ by UV-Vis spectrophotometer [14].

Cell-free extracts for xylose metabolic enzyme determination were prepared as follows. The recombinant xylose-utilizing yeasts were cultured in YPD medium containing 2% glucose for 48 h at 30°C. Cells were collected by centrifuging at 4000 rpm for 5 min and washed twice with PBS buffer. They were then resuspended in 4 ml cold PBS and disrupted by ultrasonic disruption for 15 min. Centrifuging the cell lysates at 4000 rpm for 25 min and supernatants were collected for activities determination of XR and XDH. Protein concentrations of cell-free extracts were detected using the BCA Protein Assay Kit (Beyotime, Shanghai, China). XR activity was measured by monitoring the change of NADPH at 340 nm in 100mM sodium phosphate buffer (pH 7.0) containing 0.15 mM NADPH and 200mM D-xylose. XDH activity was determinated by monitoring the production of NADH at 340 nm in 100mM Tris–HCl buffer (pH 7.0) with 1 mM $MgCl_2$, 50 mM xylitol and 5 mM NAD^+. The specific activities of the enzymes were expressed as micromoles of converted NADPH/NAD^+ per minute per milligram of protein (U/mg).

2.6 Western Blotting for Secreted Proteins

The recombinant yeast $Y6^g$/XynII and $Y6^g$/XylA were incubated at 30℃ to reach the logarithmic growth phase. Cell culture supernatants were collected and centrifuged at 4000 rpm for 15 min. The supernatants after centrifugation and binding buffer (20 mM imidazole, 20 mM phosphate buffer, 200 mM NaCl) were loaded into the Ni-NTA column (Nanomicro Technology, China) in a ratio of 1:2 (v/v). Then, proteins were washed by gravity flow with 150 ml wash buffer (30 mM imidazole, 20 mM phosphate buffer, 200 mM NaCl) before being eluted with 30 ml of elution buffer (200 mM imidazole, 20 mM phosphate buffer, 200 mM NaCl). Each sample was loaded onto a 15% SDS-PAGE to separate proteins. Then, all separated proteins were transferred to a nitrocellulose membrane and blocked using 5% skim milk powder in TBST (1 M Tris-HCl, 0.88% NaCl, 0.05% Tween20). The membrane was incubated in Anti-6×His mouse monoclonal antibody and goat Anti-Mouse IgG (H + L) antibody. Visualization was performed using enhanced chemiluminescence reagent (ECL). Immuno-probing signal was detected by ImageQuant LAS 4000mini.

2.7 Immunofluorescence Microscopy and Flow Cytometry

The extracellular surface displaying proteins were analyzed of immunological response by immunofluorescence microscopy and flow cytometry. We detected each protein element of minicellulosome by labeling special peptide tags with corresponding antigens. Cells of surface-displayed yeast were harvested by centrifugating at 3000 rpm for 5 min. The cells were resuspended with 250 μl rabbit anti-6×His tag antibody or mouse anti-Xpress tag antibody (1:1000 dilution). Added Alexa Fluor® 488-conjugated Goat anti-Mouse IgG (H + L) and Alexa Fluor® 647-conjugated goat anti-Rabbit IgG (H + L) after twice washes. Whole cell fluorescence images of the surface-displayed components were detected with a fluorescence microscope (LSM 780, Germany). The percentage of labeled cells was estimated using CSampler TM Plus (BD) [15, 16].

2.8 Ethanol Batch Fermentation

Cellulosic ethanol batch fermentation was conducted to test the ethanol production of engineered CBP-hemicellulosome yeast strain. Yeast cultures at logarithmic growth stage were centrifuged at 8000 rpm for 3 min and then transferred into the Erlenmeyer Flask, in which 50 g/l steam-exploded *Pennisetum purperum* or 10 g/l of birchwood xylan (β-D-xylopyranose) was used as the carbon source, and 15 FPU/g cellulose of Novozymes Cellic CTec2 enzyme was utilized. The prehydrolysis procedure was started up once Cellic CTec2 addition under the condition of 50°C, 200 rpm. After 6h-prehydrolysis, 1.0 g/l (wet weight) yeast cells of $Y6^g$/ScaI-XylA-XynII co-expressing XynII-SdbA and XylA-OlpA were added to the fermentation system at 35°C. The inoculation was referred to as beginning time of SSF. Total sugar and ethanol in the broths were obtained from triplicate experiments and measured according to our previous work [17]. Ethanol yield was calculated on the basis of total sugar consumed. All statistical calculations were performed for the reported data.

3. Results And Discussions

3.1 Di-CRISPR design for XR-XDH pathway

We tested Di-CRISPR at certain delta-targeting guide RNA to achieve multicopy chromosomal integration with high efficiency of reductase-xylitol dehydrogenase pathway in *S. cerevisiae*. Two xylose metabolic genes, *XYL1* and *XYL2*, were introduced into δ-integration of yeast Y6 genomes simultaneously by using CRISPR/Cas9. As expected, multicopy genome integration of heterologous xylose metabolic pathway was observed to a remarkable increase with elevated DNA levels.

The highest copy number of *XYL1* and *XYL2* for δ-integration through CRISPR/Cas9 mediation was 2.8 and 6.3, respectiv, ,whereas it was 1.6 and 3.2 for conventional delta integration. It demonstrated that the new replicative CRISPR/Cas9-mediated targeted δ-integration was effective in genome integration. As a result, the transformants with optimized protein expression were subsequently selected by combining enzyme activity analysis. As shown in Fig. 1, the yeast strain $Y6^{g}$/XR-XDH with higher copy-numbers than $Y6^{\delta}$/XR-XDH exhibited the higher enzyme activities, thus suggesting that the optimized regulation of xylose metabolic flux in *S. cerevisiae* is proportional to the efficiency enhancement of multi-copy chromosomal integration and multiplex genome engineering approach.

3.2 Construction of Cellulosome-producing CBP Reaction System

We designed an artificial hemicellulosome by mimicking the natural mechanism on the recombinant xylose-utilizing strain $Y6^{g}$ under the optimization of δ-integration CRISPR Cas9. Although some of functional cellulases are already genetically immobilized on *S. cerevisiae* for combinatorics and on-site enzyme loading, “chimeric hemicellulases and minihemicellulosome” have few been employed in “arming yeast” strategy for simultaneous hydrolysis and fermentation. As shown in Fig. 2, the displaying scaffoldin was functionally served as the integrating carrier for hemicellulase recruitment and was docked on $Y6^{g}$ cell surface via a-agglutinin anchor system. The set-up of scaffoldin can serve to enhance the quality of multi-enzymatic co-localization and also provide flexibility for adaptive assembly of chimeric components. Hence, the cellulosome-producing engineered microorganism enables us to achieve the synergistic reaction of CBP system on biomass accessibility by consolidating the simultaneous lignocellulose hydrolysis and available sugar co-fermentation. Moreover, considering the metabolic burden of host cell imparted by mini-cellulosome with the complex structur, ,we devise a CBP-enabling *S. cerevisiae* consortium, in which every engineered yeast strain could secrete or display different assembly component to be adaptive assembled on the surface of scaffoldin-displaying yeast cell.

3.3 Secreted Expression and Enzyme Assay

We constructed recombinant yeasts for expressing dockerin-fused xylanases (endoxylanase and xylosidase). The secreted expressions of full-length XynII-SdbA (29 kDa) and XylA-OlpA (92 kDa) were detected by Western-blot (Fig. 3). On the basis of docking of catalytic modules into the displaying scaffoldin, the functional enzyme activities were also determined. As shown in Table 3, two types of xylanases were examined in the cell culture supernatants of $Y6^{g}$/XylA and $Y6^{g}$/XynII, respectively. Each recombinant strain showed enzymatic activity of xylanase according to the xylooligosaccharides tested in the culture. No enzyme activity of control strain was detected.

Table 3
Enzyme activities of xylanases.

Strain	Substrate	Enzyme activity (U/ml)
Y6	1% PASC	ND
$Y6^{g}$/XylA	1% Xylan	3.13 ± 0.29
$Y6^{g}$/XynII	0.8% *p*NPX	3.46 ± 0.34

3.4 Functional Localization and Assembly of Artificial Cellulosome

With the successful expression of catalytic units, the capability of the artificial cellulosome to recruit chimeric enzyme components onto the displaying-scaffoldin via the specific binding interaction between cohesion and dockerin was further illustrated by immunofluorescence examination. The accessibility test of scaffoldin and dockerin-containing xylanase targeting with different epitope tags was performed. As shown in Fig. 4A column 3, the green immunofluorescent labeling of $Y6^g$/ScafI was detected by using goat anti-mouse IgG (H + L) conjugated with Alexa Fluor 488. This result confirmed that the displaying scaffoldin has successfully been anchored on the host cell surface. In additionally, both recombinant yeast strains of $Y6^g$/XylA and $Y6^g$/XynII were marked with brightly shining red fluorescence by goat anti-Rabbit IgG (H + L) conjugated with Alexa Fluor 647 (Fig. 4A, column 2), indicating that the two types of dockerin containing xylanase were already integrated into the scaffoldin. Finally, the relative assembling levels of these recruited enzymes were quantitatively assessed via testing the corresponding epitope by flowcytometry. As shown in Fig. 4B (upper right quadrant), positive populations were detected for all recombinant strains, which suggested that whole compositions of minicellulosomal architecture were successfully displayed on the $Y6^g$ cell surface and achieved the desired results. However, compared to docking single cellulosomal component, it should be noted that co-docking the scaffoldin and chimeric enzymes continuously on the cellulosome structure resulted in an obviously decrease in the positive populations (Fig. 4B), which reflected a reduced assembly efficiency caused by steric hindrance. Therefore, it might be necessary for us to improve the minicellulosomal machinery and organization by designing scaffoldin linker between the protein modules as well as the construction of carbohydrate binding modules (CBMs) to target appended catalytic units to substrate.

3.5 Xylan Hydrolysis and ethanol fermentation

The recombinant yeast $Y6^g$/ScafI-XylA-XynII displaying the cellulosomal structure with two types of hemicellulase was tested to determine its ability to simultaneous hydrolysis and fermentation from birchwood xylan which contains >90% xylose residues. Figure 4 shows the time course of xylan utilization and ethanol production during consolidated bio-processing process. An amount of hemicellulosic substrate was ceaselessly consumed by cellulosome-producing yeast $Y6^g$/ScafI-XylA-XynII within 96h with a slow but steady consumption rate of 0.006 g/l/h. Meanwhile, the decrease of the xylan concentration was consequently accompanied by the increase of ethanol titer. The highest ethanol concentration reached 0.61 g/l with 67.01% theoretical yield based on the consumed xylan. Throughout the whole simultaneous saccharification and fermentation, the released reducing sugar concentration was always below the detection limit, which demonstrated a desired pentose fermentability of xylose-utilizing recombinant *S. cerevisiae* strain associated with minicellulosome. However, as shown in Fig. 5, xylitol was produced unavoidably from xylose under the influence of redox imbalance in xylose reductase-xylitol dehydrogenase pathway, which was directly caused by different cofactor specificities of NAD^+-dependent XDH and NADPH-preferring in recombinant strain. Nevertheless, the results demonstrated the functional activity of chimeric xylanases and the applicability of consolidated bioprocessing-enabling yeast strain in direct hemicellulose-to-ethanol conversion.

3.6 SSCF performance from steam-exploded P. purperum

We conducted a fed-batch operation mode for cellulosic ethanol production previously [17]. We followed the process to SSCF from steam-exploded *P. purpereum* in this work, involving the adaption of yeast culture and the pre-hydrolysis prior to inoculation. The functionality of CBP-microorganism with synergistic combination of endoxylanase and xylosidase in simultaneous saccharification holocellulose and co-fermentation ethanol were further studied. As presented in Fig. 6 and Table 4, as the initial carbon source for growth and metabolism of yeast recombinant strain, an amount of glucose was released after 6h-prehydrolysis of solid liquefactions. However, the subsequent concentration of glucose during the whole fermentation process maintained a considerable low level, suggesting the robust metabolic capacity and fermentation property of yeast strain. Produced xylose derived from hemicellulose hydrolysis was accumulated before 60h, it was not used until glucose was depleted due to catabolite repression. It's worth noting that the amount of released xylose additionally affording by hemicellulosome-enabling yeast strain $Y6^g$/ScafI-XylA-XynII, led to an increase of 14.81% and

8.33%, respectively, both in ethanol productivity and substrate utilization rate, when compared to control strain. Despite the accumulation of xylitol, the maximum ethanol concentration achieved 12.88 g/l with the maximal cellulose conversion rate of 91.21% and hemicellulose conversion rate of 86.41% after 96 h (Table 4).

As the accessory enzyme for hydrolysis, as well as the supplement of commercial cellulases, xylanase could alter the macromolecular structure of lignocellulosic material and thus improve cellulose enzymatic hydrolysis by increasing access of cellulases to substrate. A xylan-degrading yeast strain by co-displaying hemicellulases on the surface of xylose-utilizing host cell has been reported previously but it did not involve the scaffoldin and minicellulosome [18]. While in recent years, increasing attentions have been focused on the heterologous expression of engineering xylanolytic mini-hemicellulosome for CBP whole-cell biocatalyst. Sun et al. successfully used the artificial cellulosome strategy to design the structures of cellulosomal modules consisting of a scaffoldin and three xylanases but did not evaluate the lignocellulolytic potential and co-fermentation property for natural lignocellulosic biomass [10]. In this work, the holocellulose-to-ethanol conversion from pretreated perennial C4 grass was achieved on the basis of incorporating the functional mini-hemicellulosome into the xylose-utilizing yeast strain under the optimization of δ-integration CRISPR Cas9. The structure of the hemicellulosome and its responsible function in SSCF bioreaction system of pretreated lignocellulose were further evaluated with the addition of commercial cellulase.

In generally, it is practical benefit in integrating catalytic units of xylanase into the multi-enzymatic formation of CBP system for enhancing biomass accessibility and cellulosic ethanol co-fermentation of pentose and hexose. On the other hand, besides the potential enzyme proximity synergy, the enhanced hydrolysis rate of holocellulose observed for the functional minicellulosome might be due to an overall effect caused by yeast cell surface-display system, secretion efficiency of exogenous enzyme, minicellulosomal machinery, and so on. Further studies are therefore required to improve the elaborated structural organization of designer hemicellulosome for the ideal consolidated bioprocessing based on simultaneous holo-cellulose saccharification and fermentation.

Table 4
Summaries of SSCF performance of engineered yeast strain.

Engineered strains	Maximum ethanol concentration (g/l)	Theoretical ethanol yield[a] (%)	Ethanol productivity (mg/l/h)	Ehanol yield (g/g)	Substrate consumption rate (g/l/h)[d]	Cellulose conversion rate[b] (%)	Hemicellulose conversion rate[c] (%)
Y6[g]/XylA-XynII	12.88	84.87	0.13	0.43	0.31	91.21	55.25
Y6[g]	11.47	86.92	0.12	0.44	0.27	86.41	-

[a] $\mathrm{Ethanolyield}(\%) = \frac{\mathrm{producedethnaol\,(g)}}{\mathrm{consumedglucose\,(g)} \times 0.51 + \mathrm{consumedxylose\,(g)} \times 0.51} \times 100\%$

b $\mathrm{Celluloseconversionyield}(\%) = \frac{\mathrm{Cellulose_s\,(g)} - \mathrm{Cellulose_R\,(g)}}{\mathrm{Cellulose_s\,(g)}} \times 100\%$

$(\mathrm{Cellulose_S}: \mathrm{cellulosefromtotalsubstrate};\ \mathrm{Cellulose_R}: \mathrm{cellulosefromfermentationresidues})$

c $\mathrm{Hemicelluloseconversionyield}(\%) = \frac{\mathrm{Hemicellulose_s\,(g)} - \mathrm{Hemicellulose_R\,(g)}}{\mathrm{Hemicellulose_s\,(g)}} \times 100\%$

$(\mathrm{Hemicellulose_S}: \mathrm{hemicellulosefromtotalsubstrate};\ \mathrm{Hemicellulose_R}: \mathrm{hemicellulosefromfermentationresidues})$

d $\mathrm{Substrateconsumptionrate}(\mathrm{g/l/h}) = \frac{\mathrm{Consumedcellulose} \times 1.1\,(\mathrm{g/l}) - \mathrm{Consumedhemicellulose} \times 1.136\,(\mathrm{g/l})}{96\,(\mathrm{h})}$

4. Conclusions

A designer hemicellulosome was successfully adaptive-assembled on the cell surface of xylose-utilizing *S. cerevisiae* under the optimization of δ-integration CRISPR Cas9. The surface-displaying scaffoldins consisted of the dockerin-containing xylosidase XynII and endoxylanase XylA without carbohydrate binding modules. The feasibility of CBP reaction system for direct simultaneous saccharification and co-fermentation from steam-exploded *P. purpereum* was evaluated. Despite the accumulation of xylitol, the maximum ethanol concentration achieved 4.77 g/l after 96 h with the maximal cellulose conversion of 97.02% and hemicellose conversion of 67.45%. These results demonstrate the applicability of designer hemicellulosome toward lignocellulose saccharification and co-fermentation in *S. cerevisiae*, and the importance of the minicellulosome-producing CBP whole-cell biocatalyst for cost-effective biofuel production.

Abbreviations

SSCF: Simultaneous saccharification and co-fermentation

CBP: Consolidated bioprocessing

XR: Xylose reductase

XDH: Xylitol dehydrogenase

Di-CRISPR: CRISPR-Cas9 mediated δ-integration

DSBs: Double stranded breaks

PGK: Phosphoglycerate kinase Promoter

XylA: Xylanase

XynII: Xylosidase

αMF: α-mature factor signal peptide

PBS: Sodium phosphate buffer

DNS: 3,5-dinitrosalicylic acid

PASC: Phosphoric acid swollen cellulose

*p*NPX: 4-nitrophenyl b-D-xylopyranoside

Declarations

Funding

This work was supported by the National Natural Science Foundation of China under Grant (No. 31971202); National Key Technology R&D Program under Grant (No. 2019YFB1503802; 2020B0101070001).

Author contributions

Han Liu, Xuxin Wang and Jiliang Du performed the experiments and wrote the manuscript. Zhuoran Kang performed the substrate pretreatment. Shen Tian and Xiushan Yang revised the manuscript and provided financial support. All authors contributed to the article and approved the submitted version.

References

1. Tubeileh A, Rennie TJ, Goss MJ. A review on biomass production from C-4 grasses: yield and quality for end-use. Curr Opin Plant Biol. 2016; 31:172–180.
2. Wang C, Li H, Xu L, Shen Y, Hou J, Bao X. Progress in research of pentose transporters and C6/C5 co-metabolic strains in *Saccharomyces cerevisiae*. Chinese journal of biotechnology. 2018; 34(10):1543–1555.
3. Hoang Nguyen Tran P, Ko JK, Gong G, Um Y, Lee SM. Improved simultaneous co-fermentation of glucose and xylose by *Saccharomyces cerevisiae* for efficient lignocellulosic biorefinery. Biotechnol Biofuels. 2020; 13(1).
4. Bhattacharya AS, Bhattacharya A, Pletschke BI. Synergism of fungal and bacterial cellulases and hemicellulases: a novel perspective for enhanced bio-ethanol production. Biotechnol Lett. 2015; 37:1117–1129.
5. Polizeli M, Rizzatti ACS, Monti R, Terenzi HF, Jorge JA, Amorim DS. Xylanases from fungi: properties and industrial applications. Appl Microbiol Biot. 2005; 67:577–591.
6. Park H, Jeong D, Shin M, Kwak S, Oh EJ, Ko JK, et al. Xylose utilization in *Saccharomyces cerevisiae* during conversion of hydrothermally pretreated lignocellulosic biomass to ethanol. Appl Microbiol Biot. 2020; 104:3245–3252.
7. Liu CG, Xiao Y, Xia XX, Zhao XQ, Peng L, Srinophakun P, et al. Cellulosic ethanol production: Progress, challenges and strategies for solutions. Biotechnol Adv. 2019; 37:491–504.
8. Smith SP, Bayer EA. Insights into cellulosome assembly and dynamics: from dissection to reconstruction of the supramolecular enzyme complex. Curr Opin Struc Biol. 2013; 23:686–694.
9. Goyal G, Tsai SL, Madan B, Dasilva NA, Chen W. Simultaneous cell growth and ethanol production from cellulose by an engineered yeast consortium displaying a functional mini-cellulosome. Microb Cell Fact. 2011; 10.
10. Sun J, Wen F, Si T, Xu JH, Zhao H. Direct conversion of xylan to ethanol by recombinant *Saccharomyces cerevisiae* strains displaying an engineered minihemicellulosome. Appl Environ Microb. 2012; 78:3837–3845.
11. Tsai SL, Dasilva NA, Chen W. Functional Display of Complex Cellulosomes on the Yeast Surface via Adaptive Assembly. Acs Synth Biol. 2013; 2:14–21.
12. Shi S, Liang Y, Zhang MM, Ang EL, Zhao H. A highly efficient single-step, markerless strategy for multi-copy chromosomal integration of large biochemical pathways in *Saccharomyces cerevisiae*. Metab Eng. 2016; 33:19–27.
13. Wood TM, Bhat KM. Methods for measuring cellulase activities. Method Enzymol. 1988; 160:87–112.
14. Nanmori T, Watanabe T, Shinke R, Kohno A, Kawamura Y. Purification and properties of thermostable xylanase and beta-xylosidase produced by a newly isolated bacillus-stearothermophilus strain. J Bacteriol. 1990; 172:6669–6672.
15. Tsai SL, Oh J, Singh S, Chen R, Chen W. Functional assembly of minicellulosomes on the *saccharomyces cerevisiae* cell surface for cellulose hydrolysis and ethanol production. Appl Environ Microb. 2009; 75:6087–6093.
16. Wen F, Sun J, Zhao H. Yeast surface display of trifunctional minicellulosomes for simultaneous saccharification and fermentation of cellulose to ethanol. Appl Environ Microb. 2010; 76:1251–1260.
17. Wang Z, Lv Z, Du J, Mo C, Yang X, Tian S. Combined process for ethanol fermentation at high-solids loading and biogas digestion from unwashed steam-exploded corn stover. Bioresource Technol. 2014; 166:282–287.
18. Katahira S, Fujita Y, Mizuike A, Fukuda H, Kondo A. Construction of a xylan-fermenting yeast strain through codisplay of xylanolytic enzymes on the surface of xylose-utilizing *Saccharomyces cerevisiae* cells. Appl Environ Microb. 2004; 70:5507–5514.

Figures

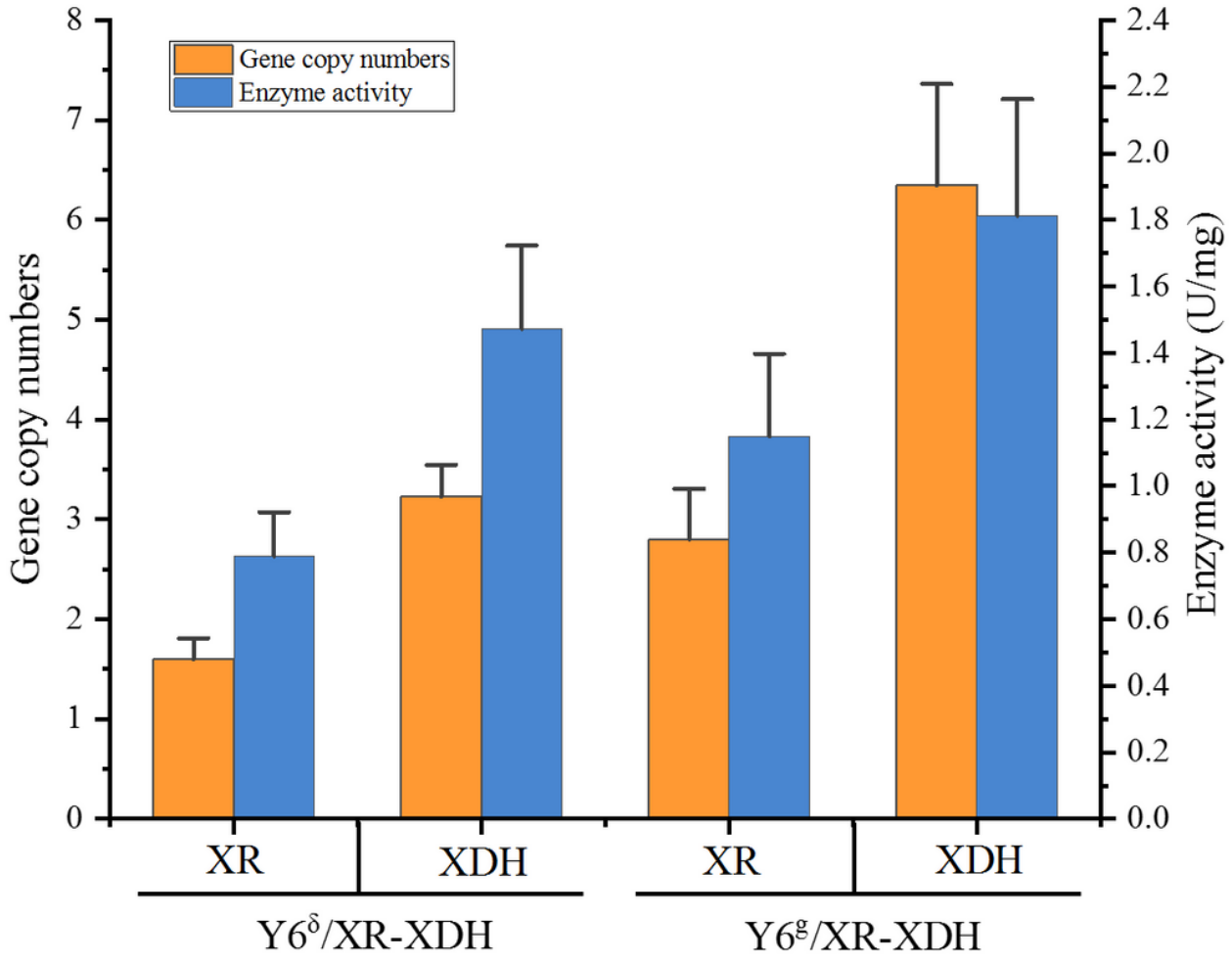

Figure 1

Gene copy number and enzyme activity of the recombinant yeast strains with δ integration and Di-CRISPR respectively.

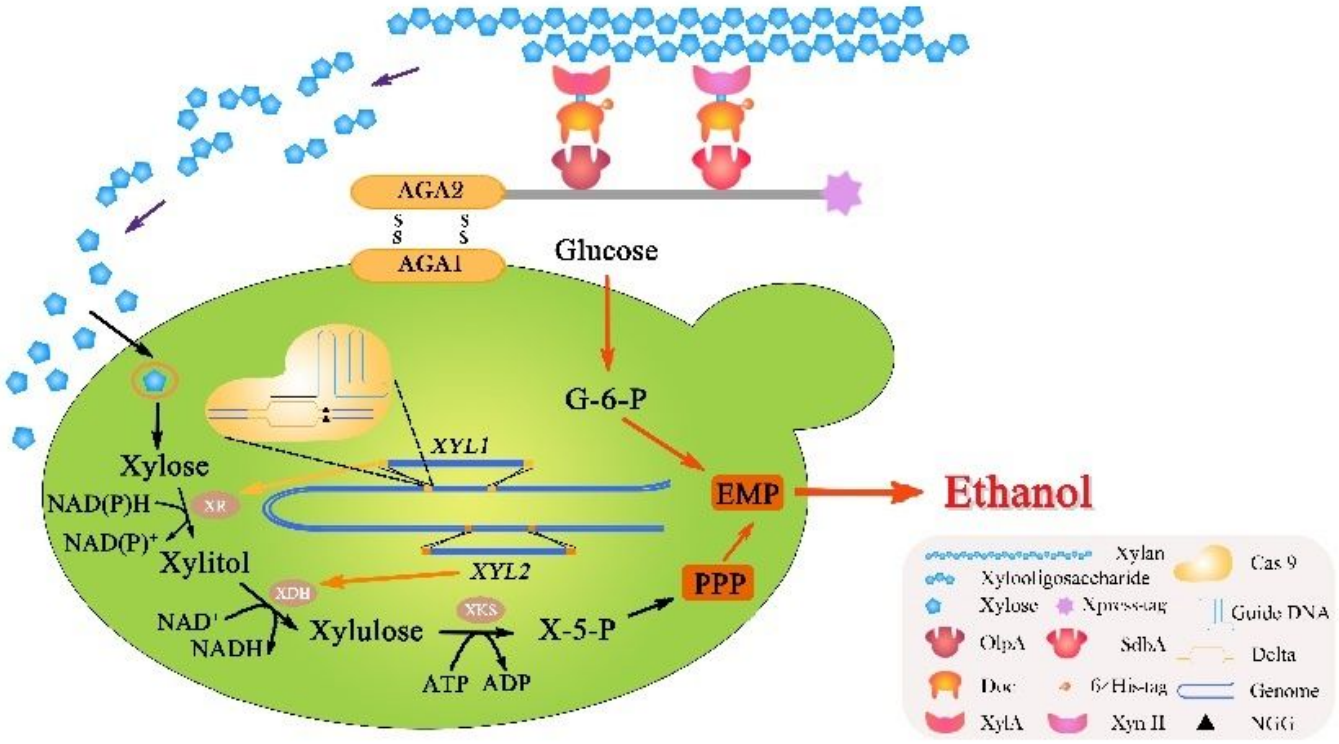

Figure 2

Schematic diagram of the designer cellulosome self-assembled on the cell surface of xylose-utilizing recombinant S. cerevisiae strain Y6^{g} under the optimization of d-integration CRISPR Cas9.

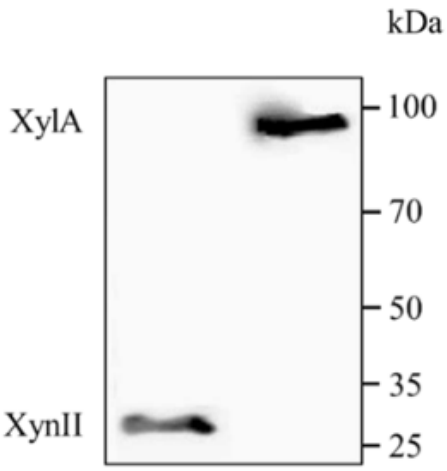

Figure 3

Western-blot analysis for protein secreted expression.

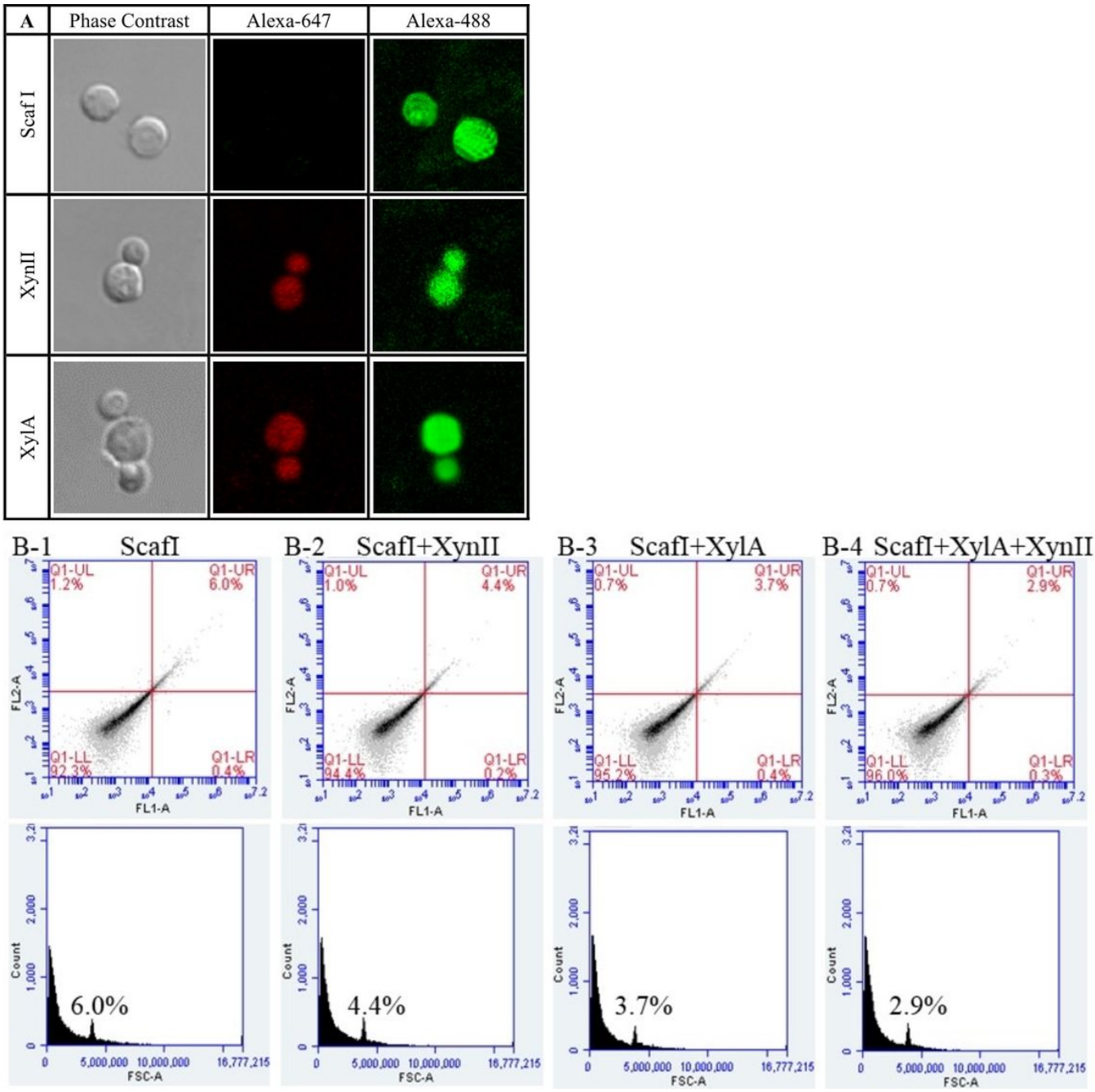

Figure 4

Functional assembly of yeast surface-displayed cellulosome. (A) Immunofluorescence micrographs of yeast whole cells displaying the anchoring scaffoldin and docked with enzymes. Cells were probed with either anti-Xpress, anti-6×His or anti-V5 and fluorescently stained with a Goat anti-Mouse IgG (H +L) conjugated with Alexa Fluor 488, Goat anti-Rabbit IgG (H+L) conjugated with Alexa Fluor 647, respectively. (B) Flow cytometric analysis of positive cells displaying different cellulosomal component.

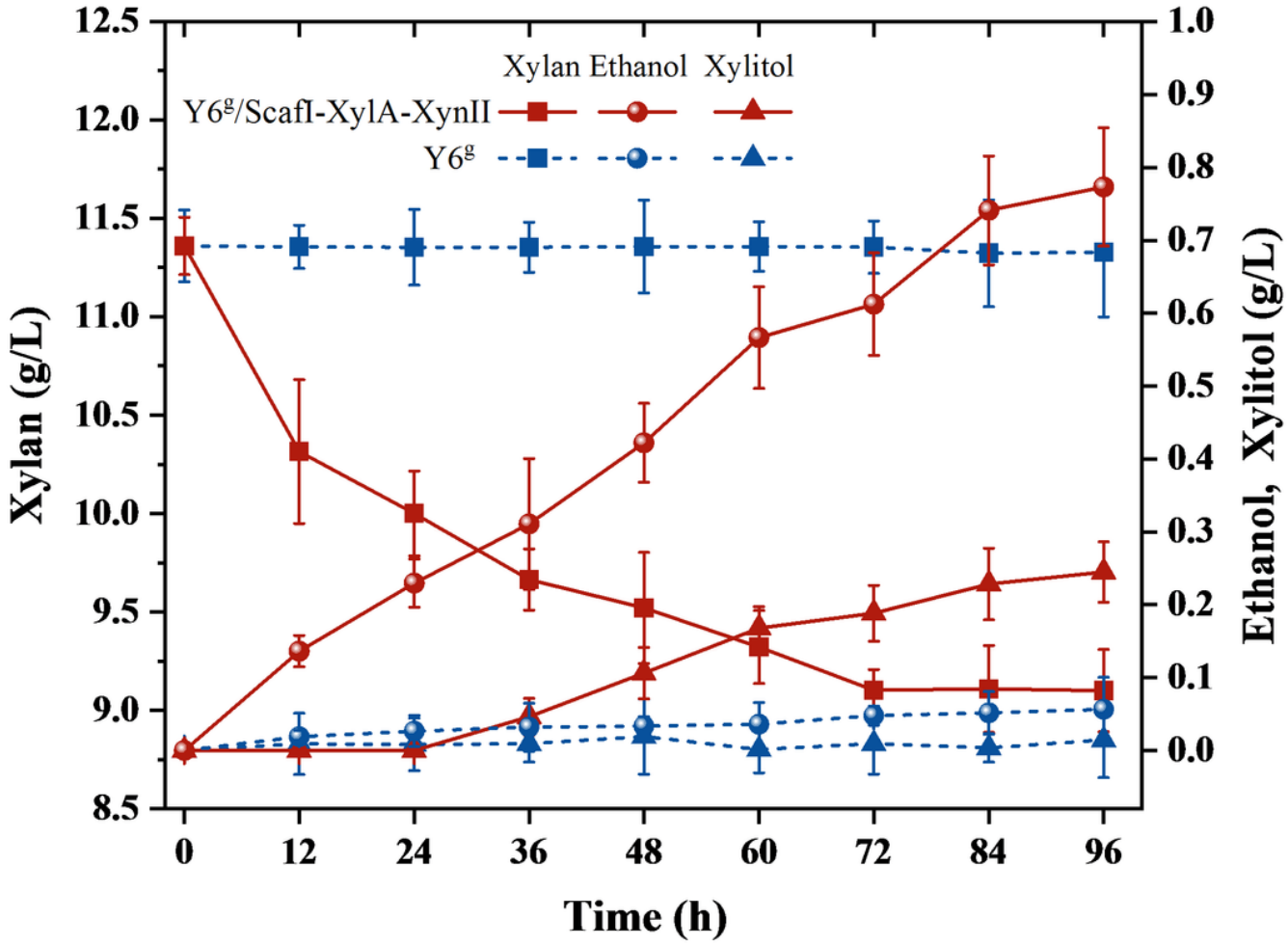

Figure 5

Time profiles of hemicellulose hydrolysis and ethanol production from birchwood xylan by using Y6^{g}/ScafI-XylA-XynII with two chimeric enzymes docking on the designer cellulosome.

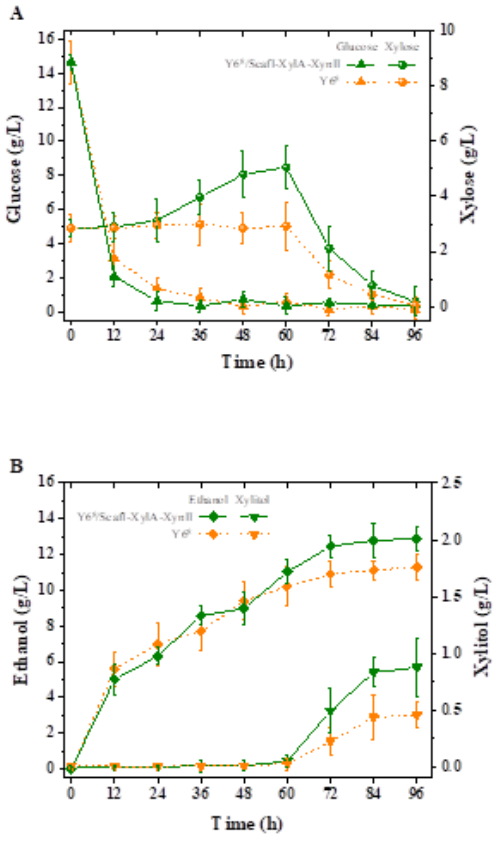

Figure 6

Time profiles of lignocellulose hydrolysis (A) and ethanol production (B) from steam-exploded *P. purpereum* after 6h pre-hydrolysis by using engineered $Y6^{g}$/ScafI-XylA-XynII displaying functional hemicellulosome.

Supplementary Files

This is a list of supplementary files associated with this preprint. Click to download.

- Supplementarymaterial.docx